MedCrave
Step into the World of Research
Material Science & Engineering International Journal

Research Article

Open Access
CrossMark

Characterization of fly ash/chitosan composites aimed for heavy metal adsorbents

Abstract

The processes of generation, management, treatment and disposal of fly ash industrial waste particles, all over the world, were considered as serious issues of solid waste. The subject of this research work was to create and to characterize the Fly ash/Chitosan composites aimed for heavy metal adsorption in polluted waters. Three different types of fly ash waste particles were used, two types supplied from EURONICKEL and one supplied from OSLOMEJ, Macedonia. The surface of the fly ash (FA) particles was modified by treated with nitric acid (HNO_3). Several types of composite adsorbents were prepared using the chitosan as a polymer matrix. The characterization of the metallurgical waste particles was performed by XRF, XRD, TGA, SEM and FTIR analysis, while the obtained composites were tested by TGA, SEM and FTIR analysis. It was observed that the structure, morphology, and some other characteristics of FA particles have been significantly changed after treatment with chitosan and it is expected that it will improve their adsorption capacity of heavy metal ions.

Keywords: fly ash, chitosan, composites, characterization

Volume 6 Issue 3 - 2022

Egzona Osmani, Iva Dimitrievska, Perica Paunovic, Anita Grozdanov
Faculty of Technology and Metallurgy, University Ss Cyril and Methodius in Skopje, Macedonia

Correspondence: Anita Grozdanov, Faculty of Technology and Metallurgy, University Ss Cyril and Methodius in Skopje, Rugjer Boskovic 16, 1000 Skopje, Macedonia, Tel +0038975303578, Email anita.grozdanov@yahoo.com

Received: September 15, 2022 | **Published:** September 26, 2022

Introduction

Water is one of the world's most abundant resources, but less than 1% of the global supply of water is available and safe for human consumption.[1] nowadays, worldwide water resources are in stress due to the presence of poisonous heavy metals in water streams.[2] Heavy metal ions in aqueous media exhibit several toxic threats to the human health as well as to the other living organisms even at low concentrations.[3] These toxic metals affect cardiovascular systems, immune, digestive system, and the normal functioning of neurological via accumulation in the soft tissues and living organisms.[4] Thus, it is important to remove heavy metal ions from waters and wastewaters before they are released to the environment.[5] Researchers worldwide have developed a number of methods such as chemical precipitation, oxidation or reduction, ion exchange, filtration, membrane separations, electrochemical treatment, reverse osmosis, adsorption, ultrafiltration, evaporation recovery, coagulation etc., for removing the toxic metals from industrial effluents before discharging into aquatic streams.[6,7] Among these methods, adsorption is known to be the most efficient, and economic method for wastewater purification and it is widely used in effluent treatment processes.

Adsorption method has various advantages over other methods as following: 1) the low generation of residues; 2) simple and easy metal recovery; 3) it produces a high-quality treated effluent suitable for reuse, 4) both of design and operation processes are simple and flexible, 5) since adsorption is sometimes reversible, so the adsorbent regeneration is possible and 6) adsorbent materials are abundant in nature.[8] A large number of natural and synthetic materials were used for the adsorption-based removal of heavy metals from wastewater[9] According to Bailey *et al.* (1999),[10] an adsorbent can be considered as cheap or low-cost if it is abundant in nature, requires little processing and is a byproduct of waste material from waste industry.[11] Adsorbents such as granulated activated Carbon, modified groundnut husk, olive stones, lignite material, bagasse and fly ash, zeolites, clays, bio sorbents, resins, peanut hull carbon, betonite, water biogas residual slurry, crude coniferous bark, modified sawdust, and sugar beet pulp are used for the removal of heavy metals from aqueous solution.[12-14] FA is suggested as a promising absorbent for removal of various pollutants.[15] Fly ash (FA) is a low cost—solid industrial waste produced from the combustion of carbon and other fossil fuels from thermal power plants, which is considered as an alternative to several commercial mineral fillers such as silica, calcium carbonate, talc, carbon black, etc. because of its easy availability and low cost.[16]

FA is a powdery material made up primarily of spherical, porous, and amorphous particles. The FA has various colour from tan to grey to black. The colour depends mainly on the amount of unburned carbon and presence of iron compounds. The size of particle is usually between 0.01 and 200 μm. Specific gravity is from 1.9 to 3.0 and the bulk density is between: 1 - 2.5 g/cm^3 and specific surface area is between 2,000 to 6,800 cm^2/g. The FA typically contains 90 - 99% inorganic material, 1-9% organic material, and up to 0.5% fluid components. The inorganic material is composed of 34 - 80% amorphous materials and 17% - 63% crystalline phases. The crystalline phases are usually: quartz, mullite, and various iron rich phases such as: hematite, goethite and calcite. The FA organic component is characterized by unburned carbon.[17] although it may contain some hazardous substances, such as heavy metals, it is widely utilized in industry in many countries. For example, in 1994, approximately 6.74 million metric tons of coal fly ash was used in the United States in cement and concrete products.[18,19] FA can also be used as a low-cost adsorbent because of its excellent specific surface area, porosity, particle size, and other natural characteristics. FA is a large porous structure exhibiting an irregular shape, with large specific surface areas and high adsorption activities.[15]

The chemical structure of FA is determined by the form of coal used in the burning process (bituminous, sub-bituminous, or lignite). Bituminous FA has a particle size of less than 0.075 nm. Sub-bituminous coal FA, on the other hand, is rougher and larger than bituminous coal FA.[20] As we already know that fly ash is a by-product material derived from the combustion of pulverized coal, therefore, the properties of fly ash is strongly depending on the characteristics of the source material, which is coal, and also the combustion process, as well as the cooling process. Owing to the rapid cooling of the material, fly ash are composed about 50-90% of the mineral matter in the form of glassy particles. Additionally, the rapid cooling in the post-combustion zone also results in the formation of spherical and amorphous particles.[21] Particle size distribution is the physical characteristic of fly ashes most strongly affecting their reactivity.[22]

The major portion of FA is mainly composed of SiO_2 and Al_2O_3 but a small amount of Fe_2O_3, Na_2O, MgO, and K_2O is also present in the material.[16,23] Fly ash seems to fulfill all the physical requirements of mineral fillers.[24] Silica is the most amount of oxide contained in fly ash, and as a source material is the main constituent of the structural skeleton of the reaction product. Alumina content in fly ash is as important as silica. The role of silica and alumina oxide is usually expressed as Si/Al ratio, where it is believed that increasing in that ratio will increase the compressive strength of product.[21] In general, FA consists of two categories refer to the total element of Si, Fe, and Al. Fly ash is classified as class C when the total content of these elements is more than 50%, and class F when it is more than 70%.[25] Class F fly ash is pozzolanic brought out from either anthracite or bituminous burning of coal. Class C ashes are pozzolanic, and cementitious produced from sub-bituminous or lignite coal burning.[26] In the recent years, the study using FA for adsorption of some heavy metal ions in wastewater has been focused.[27,28] FA is a strong and low-cost adsorbent for HMs due to its surface structure, charge, and morphology. As a result, FA, either alone or in combination with other materials is a complex substrate capable of simultaneously removing HMs.[17] In recent years, FA has been employed as a low-cost adsorbent for gas and water cleaning, but also, much efforts have been focused on used of FA in removal of heavy metals.[29]

In this study, FA samples were modified using the chitosan biopolymer matrix. Chitosan is a partially de acetylated polymer of chitin and is usually prepared from chitin by de acetylation with a strong alkaline solution. Chitosan is a low-cost biopolymer, abundant in nature and has metal sorption capability.[30] Chitosan (CS) is a polymer of particular interest in this area because it is biodegradable, bio absorbable, is non-toxic and bactericidal.[31,32] Chitosan (CS) is a polysaccharide composed of glucosamine and N-acetyl glucosamine linked with a b-1-4- glycosidic linkage (Crini et al.).[33] The uniqueness of CS molecular structure comes from the availability of amino (–NH_2) and hydroxyl (–OH) groups, which are represented active adsorption sites for the removal several of water pollutants such as dyes and metal ions.[34] Chitosan is an organic polymer coagulant aid that is non-toxic and has the function of electric neutralization and adsorption bridging. Chitosan is insoluble in water, organic solvents and aqueous bases and it is soluble in acidic media such as acetic, phosphoric, nitric, hydrochloric, perchloric acids except sulfuric one.[35] some researchers have attempted to treat polluted wastewater by using chitosan in combination with bentonite, montmorillonite, diatomite, fly ash and other materials.[36] Commercial CS's are semi-crystalline polymers and crystallinity plays an important role in adsorption efficiency.[37] The general schematic diagram for the preparation and adsorption of heavy metals ions on to FA/CS composite was shown in Figure 1.

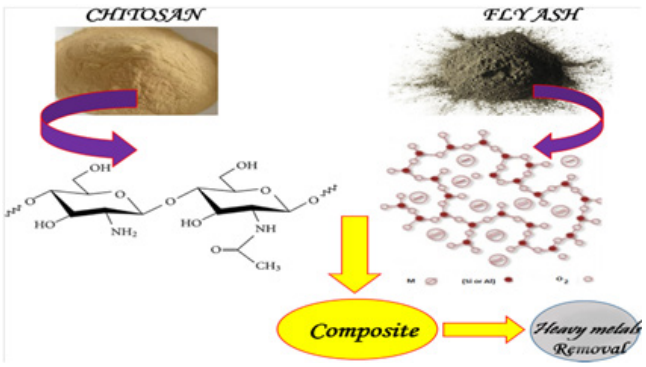

Figure 1 Schematic diagram for the preparation and adsorption of HMs ions on to FA/CS composite.

The aim of this work is to design a bio sorbent composite based on modified metallurgical waste FA particles and their combination with biopolymer chitosan.

Experimental

Materials and methods

Three different types of fly ash waste particles were used in this work, two types supplied from EURONICKEL (EN) and one supplied from OSLOMEJ (OS), Macedonia. The grey type of FA particles were obtained from OSLOMEJ coal-burning thermal power plant (marked as FA-OS). The Red brown FA waste particles were generated as a byproduct in the Installation for Ferronickel production process (marked as FA-EN), while in the next steps of ferronickel production smelting in electric arc furnace, as a waste material, the slag produced is denoted as EAFS-EN.

Modification of the Fly Ash particles.

Nitric acid (HNO_3) was used for surface modification of the FA particles. After mixing with nitric acid, the solution was heated at 100 °C for 1 h, followed by FA filtration and washing with distilled water. After the acidic treatment, the particles were immersed in 20 mL 0,1 M EDTA, stirred for 1 h and left overnight. Finally, the FA particles were filtered, washed with distilled water, and dried overnight at air oven on 100°C.

Preparation of fly ash/chitosan composites

About 0.2 g medium molecular weight of chitosan was slowly added to 200 mL of 10 wt % oxalic acid solution with stirring. The acid and chitosan form a viscous mixture (gel), which must be heated to a temperature of 40-50°C to facilitate mixing. Approximately 100 mL of the chitosan gel was diluted 2-fold with water and heated to 40-50°C.

2 g of FA particles previously treated with nitric acid and EDTA were slowly added to the diluted gel and stirred for about 36 h. The content was allowed to settle, and the clear liquid was filtered out under vacuum with Whitman 41 filter paper. The obtained composite was washed twice with DI water and dried at oven at 55°C under vacuum for

24 h. The coating process was then repeated on the once-coated FA particles to increase loading of chitosan on the FA. Excess oxalic acid in the composite was neutralized by treating with aqueous solution of NaOH 10% 200 mL. The mixture was then filtered with Whitman 41 filter paper, washed with ~ 500 mL of deionized water, and filtered. The twice-coated particles were then dried in the oven under vacuum at 55°C for about 48 h and transferred to a glass bottle for storage in a desiccator. The composites that have been prepared are: 1) FA-OS St+chitosan; 2) FA-OS NaOH+chitosan; 3) FA-EN St+chitosan; 4) FA-EN NaOH+chitosan; 5) EAFS-EN St+chitosan; 6) EAFS-EN NaOH+chitosan.

Characterization

The characterization of the metallurgical waste particles (FA-OS, FA-EN and EAFS-EN) was performed by XRF, XRD, TGA, SEM and FTIR techniques. The chemical composition of the metallurgical waste particles was determined by X-ray fluorescence (XRF) spectrometer (Model XRF ARL 9900). Mineralogical analysis was carried out by X-ray diffraction method using Philips APD 15 diffractometer, operating at CuKα-radiation. Diffraction data were scanned at rate of 0.02° s^{-1} within an angle range of 2θ = 10–80°. TGA measurements were performed using a Perkin Elmer Diamond-D7 Thermo

Citation: Osmani E, Dimitrievska I, Paunovic P, et al. Characterization of fly ash/chitosan composites aimed for heavy metal adsorbents. *Material Sci & Eng.* 2022;6(3):123–130. DOI: 10.15406/mseij.2022.06.00189

gravimetric/Differential Thermal Analyzer. The tested materials were heated at a temperature interval from 25 to 800 °C for waste materials and 25 to 500 °C for the composites, by heating rate of 20 °C min^{-1} in air atmosphere. SEM analysis of the prepared samples was done by using a Scanning Electron Microscope JEOL JSM-IT200. FTIR-ATR spectra were collected by Perkin Elmer–Spectrum 100 machine at 64 scans, in ATR mode in range from 400 cm^{-1} to 4000 cm^{-1}.

Results and discussion

Characterization of raw FA samples

The chemical compositions of the used FA waste samples determined by XRF, is shown in Table 1.

Table 1 Chemical compositions of the Raw Fly Ash samples determined by XRF

Component	FA-EN	FA-OS	EAFS-EN
SiO_2	37.5	50	53
MgO	14.5	1.5	16,9
CaO	2.3	3	2,4
Al_2O_3	1.8	30	2,0
Cr_2O_3	1	/	2,5
CoO	0.1	/	0,1
NiO	2.7	/	0,1
Fe_2O_3	30	13	14
TiO_2	/	1	/

Dominant oxides in FA-OS are: SiO_2 (50%), Al_2O_3 (30%), Fe_2O_3 (13%), CaO (3%). Dominant oxides in FA-EN are: SiO_2 (37.5%), Fe_2O_3 (30%), MgO (14.5%), NiO (2.7%). Dominant oxides in EAFS-EN are: SiO_2 (53%), MgO (16.9%), Fe_2O_3 (14%), Cr_2O_3 (2.5%). The chemical structure of FA is determined by the form of coal used in the burning process (bituminous, sub-bituminous, or lignite). According to the "American Society of Testing and Materials (ASTM C618)", FA residues is divided into two categories based on their chemical composition: "Class F and Class C".[20] The class F is characterized by a high percentage of silica (SiO_2), alumina (Al_2O_3), and iron oxide (Fe_2O_3). While the class C is characterized by a least percentage of silica (SiO_2), alumina (Al_2O_3), and iron oxide (Fe_2O_3). Class F fly ash has more amorphous alumino-silicate than class C (the amorphous state is less thermodynamically stable). Class F fly ash (FA-F) is produced as a byproduct of burning anthracite or bituminous coal, FA-C usually has cementitious properties as well as pozzolanic properties. The standard chemical requirements of ASTM C 618 include the sum of SiO_2, Al_2O_3 and Fe_2O_3 content (≥70% for Class F and between 50 and 70% for Class C) based in table 1. FA-OS is Class F (50%+30%+13%=93%); FA-EN is Class C (37.2%+1.8%+30%= 69%); EAFS-EN is Class C (53%+2.0+14%=69%). The present minerals or compounds (mineralogical analysis) in the waste materials were determined by XRD. Corresponding XRD (raw fly ash) spectra are shown in Figure 2.

FA-EN is consisted of silicates, mainly of olivine (O), quartz (Q), forsterite (F), spinel (S) and hematite (H). In many cases the color of fly ash is determined by the content of iron oxide; for example, hematite (H) gives the material a reddish tinge. FA's dominant mineral is $(Mg, Fe)_2SiO_4$ (olivine O), then $MgAl_2O_4$ (spinel S), followed by minerals in smaller amount: $MgSiO_4$ (forsterite F), Fe_2O_3 (hematite H), SiO_2 (quartz Q), and $NaAlSi_3O_8$ - $CaAlSi_2O_8$ (plagioclase P) in traces. EAFS-EN exhibits similar composition as FA-EN with olivine as a dominant mineral, then forsterite, quartz, and plagioclase in traces. The key difference between FA-EN and EAFS-EN is the presence of hematite and spinel in FA. The hematite content contributes for difference in color between these two types of waste, giving the FA-EN a reddish tint compared to the gray EAFS-EN, as shown in Figure 3. As it can be seen on the XRD spectra, FA-EN consist mainly of crystalline phases such as Quartz (SiO_2), Alumina (Al_2O_3) and Hematite (Fe_2O_3).[39]

Thermo gravimetrical analysis of the metallurgical FA waste particles is shown in Figure 4. The TG curve show difference in the thermal stability of the different FA samples. FA-OS is not stable while exposed to high temperatures, resulting with fast degradation; the sample degradation was calculated to approximately 70%, at 45 °C. FA-EN shows average stability compared to the other samples – it shows moderate stability to high temperatures, with calculated degradation to approximately 20-30%, at 52 °C. EAFS-EN shows excellent thermal stability at higher temperatures, with calculated degradation of approximately 1-2% at 98°C.

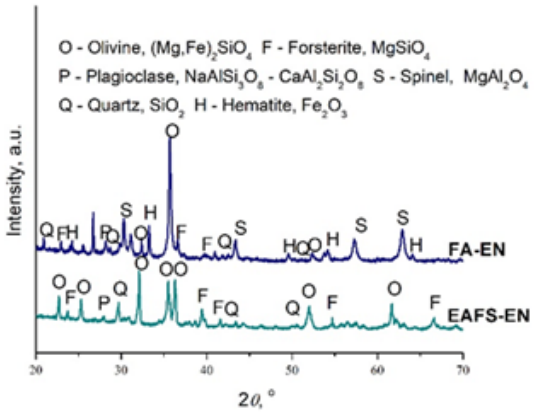

Figure 2 XRD spectra of the metallurgical waste.

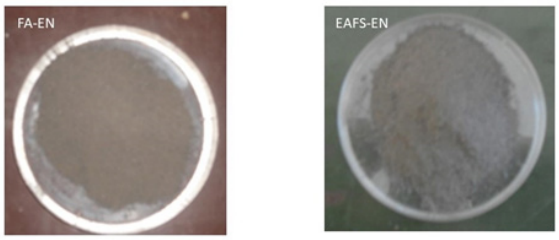

Figure 3 Images of the appearance of the metallurgical FA waste particles.

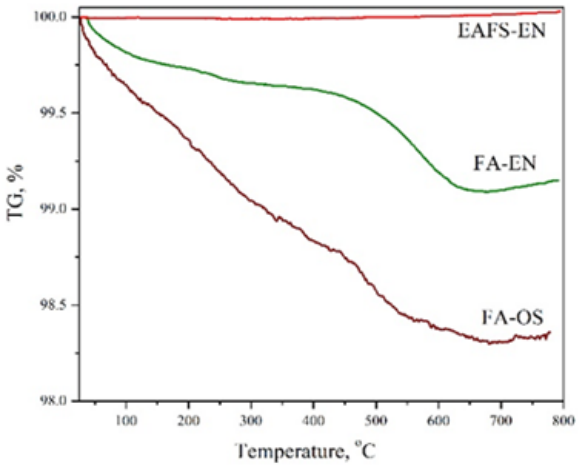

Figure 4 TGA analysis of the metallurgical waste.

Citation: Osmani E, Dimitrievska I, Paunovic P, et al. Characterization of fly ash/chitosan composites aimed for heavy metal adsorbents. *Material Sci & Eng.* 2022;6(3):123–130. DOI: 10.15406/mseij.2022.06.00189

The difference of thermal stability occurs due to the content of different oxides in different types of FA, which corresponds to degradation of the mixed oxides, i.e., silicates (olivine, forsterite and plagioclase).[40] EAFS-EN has high content of oxides as: silicate (SiO_2) with participation 53%, which has high thermal stability and high temperature ~1000 °K. Then EAFS-EN has high participation of calcits as: MgO which is present with 16.9% which also has high melting point (2852 °K), high thermal conductivity, is thermodynamically stable, and is stable at high temperatures. The same happens with FA-EN, also has a high content of MgO with a participation of 14.5%. Whereas FA-OS although has high content of SiO_2 with participation 50%, has suffered high degration in high temperatures, because has very small content of calcits as MgO (1.5%). Also FA-EN (30%) and EAFS-EN (14%) have higher amounts of Fe_2O_3, compared to FA-OS (13%). Fe_2O_3 has a high melting point of (2,849 °F), (1,565 °C) which affects the thermal stability of these wastes. The difference between FA-OS and EAFS-EN, regarding thermal stability, may also depend on the presence of quartz mineral, because the addition of quartz as a flux material lowers the temperatures of the iron ore oxidation phases.[41] FA-OS contains larger amount of quartz mineral, and smaller amount of iron oxide, vice versa to EAFS-EN, as shown in Figure 2.

Characteristic SEM images of the morphology of the waste materials, are shown in Figure 5. FA-OS is irregular form material and has surface with pores, mostly glassy (amorphous). Different shapes were found in this sample such as: oval, ellipsoid, cylinder etc. FA-EN is a material with regular spherical smooth shape, which are in different size and flat surface. EAFS-EN is irregular form material and has surface no flatted but it with layers, which look as broken.

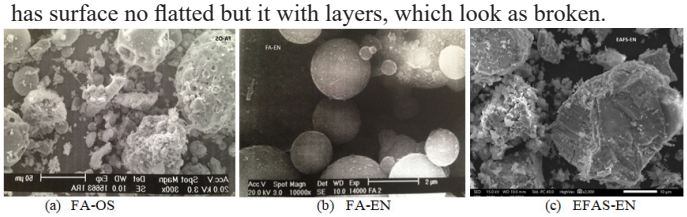
(a) FA-OS (b) FA-EN (c) EFAS-EN

Figure 5 SEM images of the metallurgical waste.

Waste materials' particle morphology is characterized using SEM, as shown in Figure 5. FA-OS exhibited as irregular shape particles with porous surface and exhibits mostly glassy (amorphous) structure. Different particle shapes were found in this sample such as: oval, ellipsoid, cylinder etc. FA-EN has spherical shape particles with smooth surface, ranging in different size. EAFS-EN shows characteristic layered structure and particles with irregular shape.

Characterization of composites

SEM–EDS analysis was carried out in order to investigate the surface morphological structure of FA-CS composites. The SEM images of FA-CS composite are shown in Figure 6. The surface morphology of FA-OS St. composites shows irregular, heterogeneous surface with different dimensions. Some ribbon shapes are also observed. It has semi crystalline structure, and the parts of the material are mainly scattered. The surface of FA-OS St. after chitosan modification has more compact pore less surface, making it a semi crystalline material.

FA-OS treated with NaOH has the same structure and shape, meaning fly ash do not change much after alkali treatment. The surface morphology of FA-EN St composites shows irregularity and roughness, compact and mainly crystal structure, appearing in large clusters, which indicates that fly ash does not change much after alkali treatment. The metallurgical waste in both cases acts as a good filler for the chitosan, achieving a suitable level of interaction with chitosan adsorbent. The surface morphology of EAFS-EN St. composites shows irregular shape and rough surface, with mainly amorphous structure which is divided into parts of different sizes, whereas EAFS-EN after NaOH treatment has amorphous structure with rough and porous surface. In all cases the fine particles of FA are combined with CS, which forms the porous particles of different sizes. This structure can play a role in the adsorption of CS and FA simultaneously, and further improve the adsorption properties of FA/CS composites.[42] The SEM-EDS analysis shows that the FA-OS composites contains the elements O, Al, Si, K which are shown in Figure 7. K is one of the basic components of chitosan shown by the analysis of the chemical composition of chitosan.[43] while the participation of dominant oxides in FA-OS composites are shown in Table 2. Based in the table we see dominant oxides are (SiO_2) with participation 68.02%; (Al_2O_3) 27.44%; and (K_2O) 4.55%. After modified of FA with chitosan we see that K_2O is a new oxide in the structure of FA modified with chitosan, compared with Raw FA. K_2O is a heavy oxide and considered a very stable and predictable oxide, thus making FA modified with chitosan a more stable material while exposed to high temperatures. The K_2O content in the system plays an important role; with increasing the K_2O content, the setting time can be increased, the compressive strength can be raised, and the fire resistance characteristics can also be improved.[43]

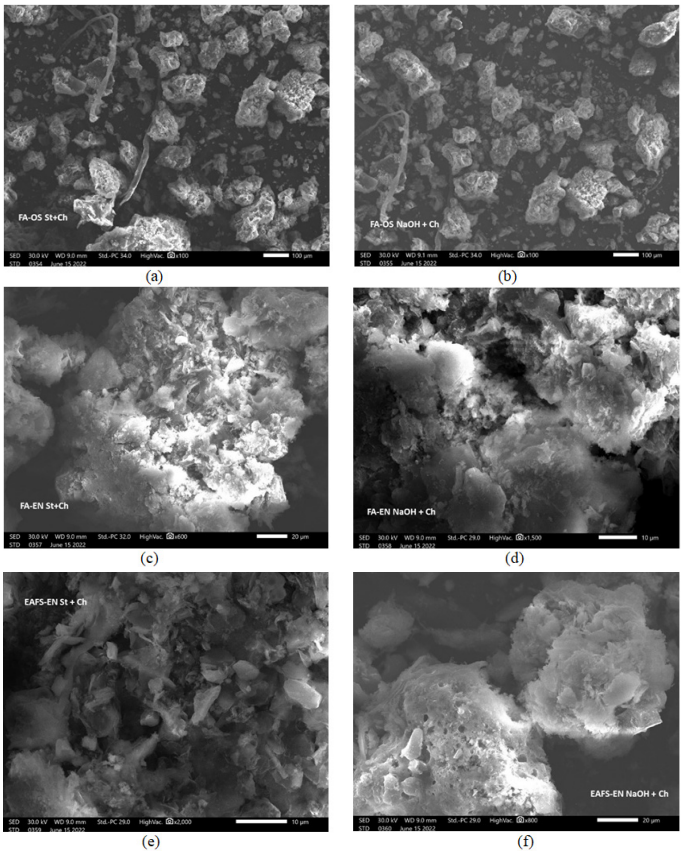

(a) (b) (c) (d) (e) (f)

Figure 6 SEM images of the FA modified with chitosan.

Characteristic TGA curves for the obtained composites are shown in Figure 8, while the degradation temperatures, *Td*, and DTG data were presented in Table 3. The samples exhibited three stages of weight loss, except the FA-OS NaOH+Ch composite. In the first stage, FA-OS St.+Ch has a remaining mass of 99.0%, then 96.5%, followed by 86.1% at the end, with a decomposition temperature of 67.5 °C, 273.9 °C and 429.4 °C. FA-OS NaOH+Ch composite shows remaining mass of 99.20% in the first stage, and 96.21% in the second

Citation: Osmani E, Dimitrievska I, Paunovic P, et al. Characterization of fly ash/chitosan composites aimed for heavy metal adsorbents. *Material Sci & Eng.* 2022;6(3):123–130. DOI: 10.15406/mseij.2022.06.00189

stage with a decomposition temperature of 73.2 °C and 287.4 °C, respectively. The remaining mass in the first stage for FA-EN St.+Ch composite is 99.43%, followed by 97.46% in the second, and 88.46% in the third stage with a decomposition temperature of 65.1 °C, 288.9 °C, and 673.3 °C, respectively. Remaining mass for FA-EN NaOH+Ch is 99.43%, 97.67%, and 88.73% with a decomposition temperature of 63.4 °C, 288.0 °C and 677.5 °C. EAFS-EN St.+Ch composite shows remaining initial mass of 98.48% in the first, 91.17% in the second, and 75.3% in the third stage with a decomposition temperature of 102.7 °C, 289.7 °C, and 511.0 °C.

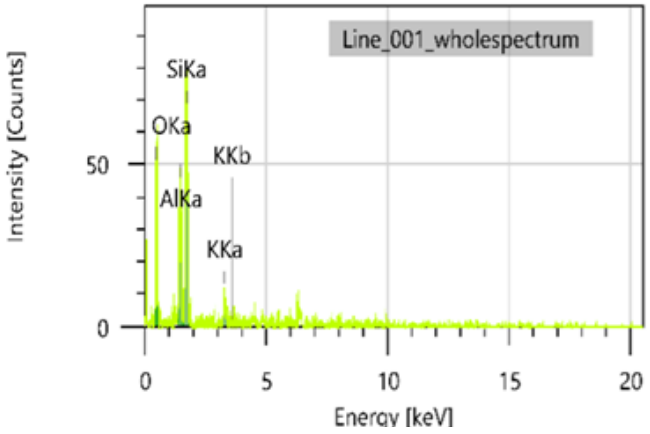

Figure 7 SEM-EDS chemical analysis for FA-OS chitosan composites.

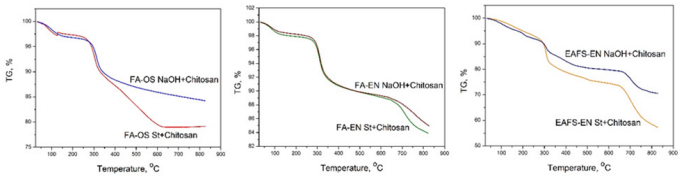

Figure 8 TGA curves for the studied composites: 1) FA-OS St+chitosan; 2) FA-OS NaOH+chitosan; 3) FA-EN St+chitosan; 4) FA-EN NaOH+chitosan; 5) EAFS-EN St+chitosan; 6) EAFS-EN NaOH+chitosan.

Table 2 oxides on the surface and their mass and molar %

Chemical formula	Line	Mass%	Mol%	Cations
O	K			
Al2O3	K	27.44 ± 2.26	18.56 ± 1.53	4.14
SiO2	K	68.02 ± 4.08	78.11 ± 4.69	8.71
K2O	K	4.55 ± 0.75	3.33 ± 0.55	0.74
Total		100	100	
Line_001_wholespectrum			Fitting ratio 0.5587	

Table 3 Degradation temperatures, *Td*, for FA based Chitosan composites

SAMPLE	Td_1, °C, %	Td_2 °C, %	Td_3, °C, %	DTG_1 °C, mg min^{-1}	DTG_2 °C, mg min^{-1}	DTG_3 °C,mg min^{-1}
	67.5	273.9	429.4	92.6	307.4	519.7
1) FA-OS St.+ Ch						
	99,0	96.5	86.1	164.5	854.3	212.2
2) FA-OS						
	73.2	287.4		104.3	315.8	
NaOH+Chit			/			/
	99,20	96.21		0.242	1.367	
	65.1	288.9	673.3	88.1	314.0	717.7
3) FA-EN St.+Ch						
	99,43	97.46	88.46	0.143	0.998	0.292
4) FA-EN	63.4	288.0	677.5	85.1	316.4	764.4
NaOH+Ch	99.43	97.67	88.73	88.9	787.3	150.6
	102.7	289.7	511.0	524,7	56,7	100,5
5) EAFS-EN St+Ch						
	98.48	91.17	75.3	95,7	15,7	17,9
6) EAFS-EN	190.1	289.5	672.7	108	206	397
NaOH + Ch	94.4	90.7	79.12	242	369	302

The initial mass remaining in the first stage for EAFS-EN NaOH+Ch is 94.4%, followed by 90.7%, and 79.12% with a decomposition temperature of 190.1 °C, 289.5 °C, and 672.7 °C. The outcomes revealed that all samples showed decomposition temperatures for the first and second stage that have matched those obtained by chitosan-based films.[44] It has been described that the weight loss due to the decomposition of CH starts at 240 °C and reaches a maximum at 380 °C, with a 41.4% weight loss,[45] and the main weight loss seen at 304 °C for CH is assigned to CH degradation.[46,47] The rate of mass loss is calculated using the DTG peak height at any temperature.

Citation: Osmani E, Dimitrievska I, Paunovic P, et al. Characterization of fly ash/chitosan composites aimed for heavy metal adsorbents. *Material Sci & Eng.* 2022;6(3):123–130. DOI: 10.15406/mseij.2022.06.00189

The first peak in the DTG curve, for sample 1) FA-OS St +Ch with maximum decomposition rate at 92.6°C, is associated with weight loss of 164.5 mg*min-1 which happens due to moisture vaporization indicating the hygroscopic nature of CS composites.[48] The second peak, with maximum decomposition rate at 307.4°C and a weight loss of 854.3 mg*min^{-1}, is associated with the release of material from the non-acetylated and the acetylated units of the polymer.[49] The third peak with maximum decomposition rate at 519.7 C and a weight loss of 212.2 mg*min^{-1}, which corresponds to the partial oxidation and decomposition of glucosamine residues followed by charring.[49,50]

The first peak in the DTG curve, for sample 2) FA-OS NaOH+Ch with maximum decomposition rate at 104.3 °C, is associated with weight loss of 0.242 mg*min-1, while the second with maximum decomposition rate at 315.8 C has a weight loss of 1.367 mg*min^{-1}. The first peak in the DTG curve, for sample 3) FA-EN St.+Ch with maximum decomposition rate at 88.1°C, is associated with weight loss of 0.143 mg*min^{-1}, the second with maximum decomposition rate at 314.0°C, is associated with weight loss of 0.998 mg*min^{-1} and the third with maximum decomposition rate at 717.7°C, has a weight loss of 0.292 mg*min^{-1}. The first peak in the DTG curve, for sample 4) FA-EN NaOH+Ch with maximum decomposition rate at 85.1°C, is associated with weight loss of 88.9 mg*min^{-1}, the second with maximum decomposition rate at 316.4°C has a weight loss of 787.3 mg*min^{-1} and the third with maximum decomposition rate at 764.4°C, has a weight loss of 150.6 mg*min^{-1}. The first peak in the DTG curve, for sample 5) EAFS-EN St.+Ch with maximum decomposition rate at 524.7°C, is associated with weight loss of 95.7 mg*min^{-1}, the second with maximum decomposition rate at 56.7°C has a weight loss of 15.7 mg*min^{-1} and the third with maximum decomposition rate at 100.5°C, has a weight loss of 17.9 mg*min^{-1}. The first peak in the DTG curve, for sample 6) EAFS-EN NaOH+Ch with maximum decomposition rate at 108°C, is associated with weight loss of 242 mg*min^{-1}, the second with maximum decomposition rate at 206°C has a weight loss of 369 mg*min^{-1} and the third with maximum decomposition rate at 397°C, has a weight loss of 302 mg*min^{-1}. Based on the data extracted from TGA curves of the studied composites, shown in Figure 8, it can be concluded that EAFS-EN based composite is not stable, FA-OS based composite is moderately stable, whereas composite with FA-EN is most stable while exposed on high temperatures. Figure 9 shows the TGA curves for initial FA based composites with chitosan, while Figure 10 shows TGA curves for NaOH treated FA based composites.

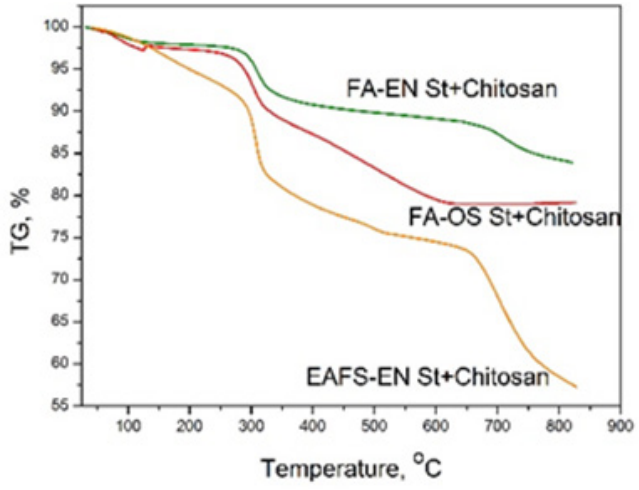

Figure 9 TGA curves for the FA based composites non treated with NaOH.

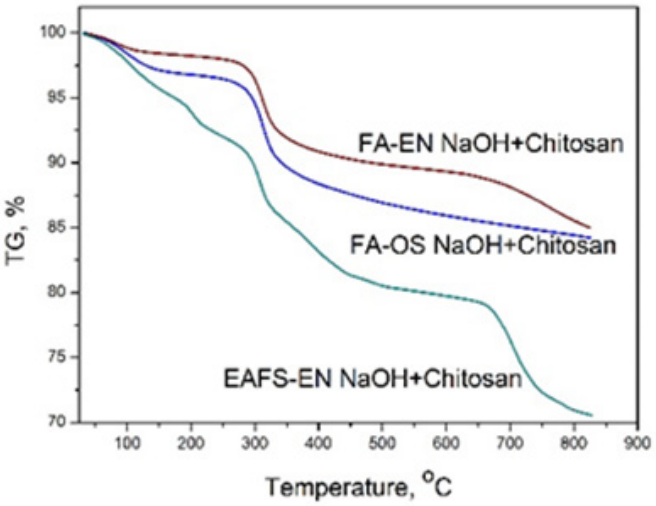

Figure 10 TGA curves for the FA based composites treated with NaOH.

The spectra of the raw fly ash are shown in Figure 11. The asymmetric, symmetric stretching, and bending vibrations of Si-O-Si group in the FA particles correspond at 1070 cm^{-1}.[51,52] Figure 12 shows the FTIR spectra of fly ash/chitosan composites. The broad band in the region between 3400-3000 cm^{-1} indicates stretching vibrations for surface OH groups of silanol groups (-Si-OH) and surface-adsorbed water molecules. The broadness of this band indicates the presence of strong hydrogen bonding,[53,54] particularly pronounced in (e-f) spectra. Peaks appearing around 2354 cm^{-1} are attributed to valent O-H stretching and 2335 cm^{-1} is responsible for H-SiO3 vibration.[54]

A peak around 1607 cm^{-1} is attributed to deformation bending vibration (δO-H) of water molecule.[54] Comparing the spectra, changes in the region 1700-450 cm^{-1} are observed. In the high-frequency region (1200-650 cm^{-1}), the broad band with strong intensity centered at around 1000 cm^{-1} is assigned to the Si(Al)–O–Si valent asymmetric stretch. This band is typical of the spectra of silicate glasses, and its frequency depends slightly on the state of hydration, non-bridging oxygen site (NBO) concentration and Al content.[55] The broadening of the band around 1000 cm^{-1} in the FA/chitosan systems is a result of bond vibrations overlapping. This region consists of bands at 1066 and 1028 cm^{-1} which correspond to C-O stretching and originate from chitosan.[56] The origin of the fly ash contributes for slight shifting of the band towards lower frequencies. This phenomenon may indicate formation of a new product (amorphous alumino silicate gel phase) due to the dissolution of the fly ash amorphous phase in strong alkaline activator – NaOH.[57] The appearance of new bands at lower frequencies (760-560 cm^{-1}) is assigned to the symmetric stretching vibrations of Si–O–Si and Al–O–Si, which are referred to the formation of amorphous to semi-crystalline alumino silicate materials.[58] The obtained spectra of fly ash show band located at about 464 cm^{-1}, ascribed to bending vibrations of Si–O–Si and O–Si–O bonds which is hardly affected, indicating that quartz is almost chemically inert in strong alkaline activators.[58] The broad bands originating from O-H and H-O-H vibrations of surface-adsorbed water molecules are present only in the (a-b) samples. The broad band around 1000 cm^{-1} present in the FA/chitosan systems, tends to shift to higher frequencies (1060-1040 cm^{-1}) and sharper peak shape. The narrow band is a result of the absence of characteristic C-O stretching vibrations, present in the chitosan.

Citation: Osmani E, Dimitrievska I, Paunovic P, et al. Characterization of fly ash/chitosan composites aimed for heavy metal adsorbents. *Material Sci & Eng.* 2022;6(3):123–130. DOI: 10.15406/mseij.2022.06.00189

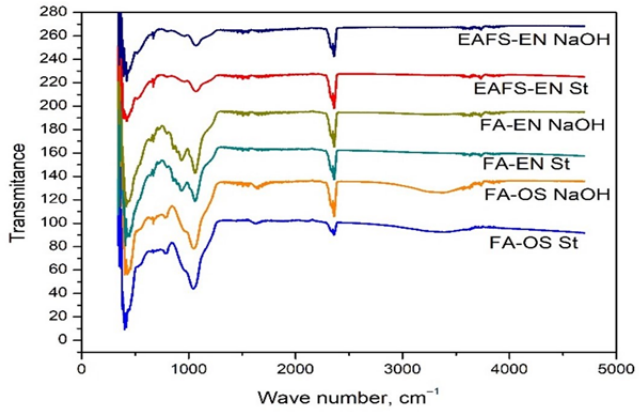

Figure 11 FTIR spectra of the raw fly ash:

1) FA-OS St; 2) FA-OS NaOH; 3) FA-FENI St; 4) FA-FENI NaOH; 5) EAFS St; 6) EAFS NaOH.

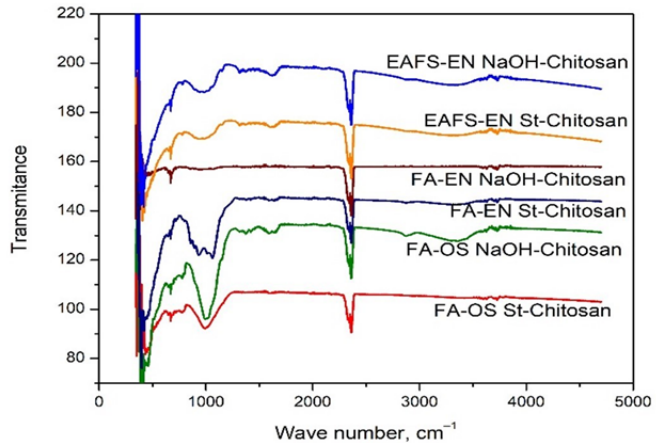

Figure 12 FTIR spectra of fly ash/chitosan systems.

Conclusions

For this study, three types of waste materials were used: FA-OS, FA-EN, and EAFS-EN. It was found that the structure, morphology, and some other characteristics of FA particles have been changed significantly after modification and their mixing with chitosan polymer matrix. The highest thermal stability was exhibited by EAFS-EN because has high content of oxides as: silicate (SiO_2) with participation 53%, and high content of calcites as: MgO which is present with 16.9% that are stable at high temperatures. While from the composites systems, EAFS-EN NaOH + Ch is the weakest, and not stable in high temperature. FA-EN NaOH + Ch is the most stable material at higher temperatures. The SEM-EDS analysis shows that the FA-OS composites contains the elements O, Al, Si, K. After modified of FA with chitosan, it was found that K_2O is new oxide in the structure of FA-OS NaOH+Ch system, compared with raw FA. K_2O is a heavy oxide and considered a very stable and predictable oxide, thus making FA-OS NaOH+Ch systems a more stable material in high temperature.

Conflicts of interest

Authors declare that there is no conflict of interest.

Acknowledgements

None.

Funding

None.

References

1. Adeleye AS, Conway JR, Garner K, et al. Engineered nanomaterials for water treatment and remediation: costs, benefits, and applicability. *Chem. Engineering Journal*. 2016;286:640–662.
2. Khalil U, Shakoor BM, Shafaqat A, et al. Adsorption-reduction performance of tea waste and rice husk biochars for Cr(VI) elimination from wastewater. *Journal of Saudi Chemical Society*. 2020;24:799–810.
3. Kumar M, Chung JS, Hur SH. Graphene composites for lead ions removal from aqueous solutions. *Appl. Sci.* 2019;9(14):2925.
4. Mirzaee AS, Jaafarzadeh N, Martinez SS, et al. Simultaneous adsorption of heavy metals from aqueous matrices by nanocomposites: A first systematic review of the evidence. *Environmental Health Engineering and Management Journal*. 2022;9(1):9–14.
5. Kılıc M, Kırbıyıkb C, Özge C, et al. Adsorption of heavy metal ions from aqueous solutions by bio-char, aby-product of pyrolysis. *Applied Surface Science.* 2013;283:856–862.
6. Shwetha K, Nagarajappa DP, Mamatha M. Removal of copper from simulated wastewater using pongamia pinnata seed shell as adsorbent. *IJERA.* 2014;6:271–282.
7. Haitham A El-A, Abdel MMAI, Mangood AH, et al. Sesame husk as adsorbent for copper(ii) ions removal from aqueous solution. *Journal of Geoscience and Environment Protection*. 2017;5:109–152.
8. Haitham A El-A, Abdel MMAI, Mangood AH. Removal of Copper(II) and Cadmium(II) ions from aqueous solution by adsorption on modified almond shells. *International Journal of Engineering & Technology*. 2019;19:5.
9. Nayab S, Baig H, Ghaffar A, et al. Silica based inorganic–organic hybrid materials for the adsorptive removal of chromium. *RSC Adv*. 2018;8(42):23963–23972.
10. Bailey. Water considerations for container production of plants. *Water.* 1999.
11. Wan Ngah WS, Hanafiah MAKM. Removal of heavy metal ions from wastewater by chemically modified plant wastes as adsorbents: A review. *Bioresource Technology*. 2008;99(10):3935–3948.
12. Atieh MA, Bakather OY, Al-Tawbini B, et al. Effect of carboxylic functional group functionalized on carbon nanotubes surface on the removal of lead from water. *Bioinorganic Chemistry and Applications*, 2010;9.
13. Sekar M, Sakthi V, Rengaraj S. Kinetics and equilibrium adsorption study of lead (II) onto activated carbon prepared from coconut shell. *J Colloid Interface Sci*. 2004;279(2):307–313.
14. Shifeng L, Fang Q, Min X, et al. In situ synthesis of layered double hydroxides on γ-Al 2 O 3 and its application in chromium(VI) removal, *Water Sci Technol*. 2017;75(5-6):1466-1473.
15. Jun CG, Sam KY, Nag JC. Application of fly ash as an adsorbent for removal of air and water pollutants. *Appl Sci*. 2018;8(7):1116.
16. Trong VM, Tuan VM, Chinh NT, et al. Characterization of fly ash modified with vinyltriethoxysilane. *J. Nanosci. Nanotechnol.* 2015;15(8):5905–5909.
17. Korniejenko K, Halyag NP, Mucsi G. Fly ash as a raw material for geopolymerisation – chemical composition and physical properties. *IOP Cof Series: Materials Science and Engineering.* 2019;706.
18. Katal R, Hasani E, Farnam M, et al. Charcoal ash as an adsorbent for ni(ii) adsorption and its application for wastewater treatment. *J. Chem Eng Data*. 2012;57(2):374−383.

19. Manz OE. Coal fly ash: a retrospective and future look. *Fuel.* 1999;78(2):133–136.

20. Uyiosa OA, Kingsley EU, Onyancha RB, et al. Fly ash-based adsorbent for adsorption of heavy metals and dyes from aqueous solution: a review. *Journal of Materials Research and Technology*, 2021;14:2751–2774.

21. Wattimena OKA, Hardjito D. A review on the effect of fly ash characteristics and their variations on the synthesis of fly ash based geopolymer. *AIP Conference Proceedings*. 2017;1887(1).

22. Fernandez-Jimenez A, Palomo A. Characterisation of fly ashes. potential reactivity as alkaline cements. *Fuel.* 2003;82(18):2259–2265.

23. Uyiosa OA, Kingsley EU, Onyancha RB, et al. Fly ash-based adsorbent for adsorption of heavy metals and dyes from aqueous solution: a review. *Journal of Materials Research and Technology*, 2021;14:2751–2774.

24. Bohara N, Tamrakar GBS. A study of effect of filler contents and filler types in marshall stability and flow value in asphalt concrete. *Proceedings of IOE Graduate Conference*. 2017;5:2350–8914.

25. Fauzi A, Nuruddin MF, Malkawia AB, et al. Study of fly ash characterization as a cementitious material. *Procedia Engineering*. 2016;148:487– 493.

26. Alterary SS, Marei NH. Fly ash properties, characterization, and applications: A review. *Journal of King Saud University – Science*. 2021;33(6).

27. Nguyen TC, Tran TM, Nguyen TTT, et al. Using fly ash treated by NaOH and H_2SO_4 solutions for Hg^{2+} and Cd^{2+} ion adsorption. *Vietnam Journal of Chemistry, International Edition*. 2017;55(2):196–201.

28. Visa M, Duta A. Methyl-orange and cadmium simultaneous removal using fly ash and photo-fenton systems. *Journal of Hazardous Materials*. 2013;244-245:773-779.

29. Pandey S, Tiwari S. Facile approach to synthesize chitosan basedcomposite—Characterization and cadmium(II) ion adsorption studies. *Carbohydrate Polymers*. 2015;134:646–656.

30. Copello GJ, Varela F, Martınez Vivot R, et al. Immobilized chitosan as biosorbent for the removal of Cd(II),Cr(III) and Cr(VI) from aqueous solutions. *Bioresource Technology*. 2008;99:6538–6544.

31. Corradini E, de Moura MR, Mattoso LHC. A preliminary study of the incorparation of NPK fertilizer into chitosan nanoparticles. *eXPRESS Polymer Letters*. 2010; 4:8:509–515.

32. Kaczmarek H, Zawadzki J. Chitosan pyrolysis and adsorption properties of chitosan and its carbonizate. *Carbohydr Res*. 2010;345(7):941–947.

33. Crini G, Badot PM. Application of chitosan, a natural aminopolysaccharide, for dye removal from aqueous solutions by adsorption processes using batch studies: A review of recent literature. *Progress in poly sci*. 2008;33(4):399–447.

34. Jawad AH, Abd Malek NN, Abdulhameed AS, et al. Synthesis of magnetic chitosan-fly ash/fe3o4 composite for adsorption of reactive orange 16 dye: optimization by box–behnken design. *Journal of Polymers and the Environment*. 2020;28:1068–1082.

35. Adamczuk A, Kołodyńska D. Fly ash coated chitosan as efficient adsorbent for removal of heavy metal ions from waters and waste waters. *Engineering*. 2015.

36. Jiang C, Wang R, Chen X, et al. Preparation of chitosan modified fly ash under acid condition and its adsorption mechanism for Cr(VI) in water. *J Cent South Univ.* 2021;28:1652−1664.

37. Trung NT, Sakaguchi Y, Nagahara H, et al. Stereo SLAM using two estimators. *IEEE explore.* 2006.

38. Govindan S, Nivethaa EAK, Saravanan R, et al. Synthesis and characterization of chitosan–silver nanocomposite. *Appl Nanosci.* 2012;2:299–303.

39. Saakshy KS, Gupta AB, Sharma AK. Fly ash as low cost adsorbent for treatment of effluent of handmade paper industry Kinetic and modelling studies for direct black dye. *Journal of Cleaner Production.* 2015;112:1227–1240.

40. Paunović P, Grozdanov A. Circular economy applied to metallurgical waste: use of slags and fly ash from the ferronickel industry in the production of eco-friendly composites. *Journal of Sustainable Metallurgy*, 2022;8:815–824.

41. Haizea PB, Zuluaga MC, Ortega LA, et al. Mineralogical characterization of slags from the oiola site (biscay, spain) to assess the development in bloomery iron smelting technology from the roman period to the middle ages. *Minerals*. 2020;10(4):321.

42. Beigang L, Shuangyan H, Rui T. Adsorption of acid carmoisine b by fly ash/ chitosan composite. *Materials Science Forum*. 2016;847:224–229.

43. Cheng TW, Chiu JP. Fire-resistant geopolymer produced by granulated blast furnace slag. *Minerals Engineering*. 2003;16(3):205–210.

44. Seham SA, Narguess HM. New isolated shrimp (litopenaeus setiferus) chitosan-based films loaded with fly ash for antibacterial evaluation. *Polymers.* 2022;14(10):2099.

45. Neto CGT, Giacometti GA, Job AE, et al.Thermal analysis of chitosan based networks. *Carbohydrate polymers.* 2005;62(2):97–103.

46. Abugoch LE, Tapia C, Villamán MC, et al. Characterization of quinoa proteinechitosan blend edible films. *Food Hydrocolloids*. 2011;25(5): 879–886.

47. Zhang ZH, Zeng ZHX, Xiong XY, et al. Enhancing mechanical properties of chitosan films via modification with vanillin. *International Journal of Biological Macromolecules.* 2015;81:638–643.

48. Akshata GP, Poornachandra S, Gumageri R, et al. Chitosan composites reinforced with nanostructured waste fly ash. *J Mater Cycles Waste Manag*. 2016;19:870–883.

49. Nieto JM, Penichea C. Characterization of chitosan by pyrolysis-mass spectrometry, thermal analysis and differential scanning calrimetry. *Thermochimica Acta.* 1991;179:63–68.

50. Sarat KS, Satyabrata D, Sudhir KK, et al. Thermal and oxygen barrier properties of chitosan bionanocomposites by reinforcement of calcium carbonate nanopowder. *J Mater Sci Technol.* 2014;30(8)1–5.

51. Thuy CN, Trang DMT, Van BD, et al. Using modified fly ash for removal of heavy metal ions from aqueous solution. *Journal of Chemistry*. 2020.

52. Plinio I, Falcaro P. Order-disorder transitions and evolution of silica structure in self-assembled mesostructured silica films studied through ftir spectroscopy**.** *J Phys Chem B***.** 2003;107(20):4711–4717.

53. Chitralekha K, Ashu R. Synthesis of a nano-crystalline solid acid catalyst from fly ash and its catalytic performance. *Fuel.* 2008;87(13-14):2886–2892.

54. Stuti K, Sakshi K, Sharma A, et al. Surface modification of fly ash by thermal activation: a dr/ftir study. *International Research Journal of Pure & Applied Chemistry*. 2013;3(4):299–307.

55. Zuhua Z, Wang H, Provis JL. Quantitative study of the reactivity of fly ash in geopolymerization by FTIR. *Journal of Sustainable Cement-Based Materials*. 2012;1(4):154–166.

56. Moacir FQ, Melo KRT, Sabry DA, et al. Does the use of chitosan contribute to oxalate kidney stone formation. *Mar drugs*. 2015;13(1):141–158.

57. Mohd MABA, Kamarudin H, Mohamed B, et al. Fly ash-based geopolymer lightweight concrete using foaming agent. *Int J Mol Sci.* 2012;13:7186-7198.

58. Panias D, Giannopoulou IP, Perraki T. Effect of synthesis parameters on the mechanical properties of fly ash-based geopolymers. *Colloids and Surfaces A: Physicochem. Eng. Aspects*. 2007;301(1-3):246–254.

Citation: Osmani E, Dimitrievska I, Paunovic P, et al. Characterization of fly ash/chitosan composites aimed for heavy metal adsorbents. *Material Sci & Eng.* 2022;6(3):123–130. DOI: 10.15406/mseij.2022.06.00189